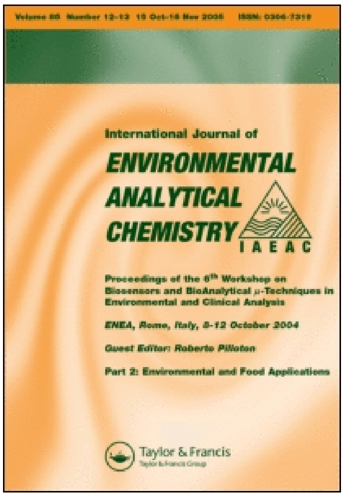

International Journal of Environmental Analytical Chemistry
Publication details, including instructions for authors and subscription information:
http://www.informaworld.com/smpp/title~content=t713640455

Solid-phase microextraction as a powerful tool in photochemical studies

Marta Lores[a]; Lucía Sánchez-Prado[a]; María Llompart[a]; Carmen García-Jares[a]; Rafael Cela[a]
[a] Departamento de Química Analítica, Nutrición y Bromatología, Facultad de Química, Instituto de Investigación y Análisis Alimentario (IIAA), Universidad de Santiago de Compostela, santiago de composa, Spain

To cite this Article Lores, Marta , Sánchez-Prado, Lucía , Llompart, María , García-Jares, Carmen and Cela, Rafael(2005) 'Solid-phase microextraction as a powerful tool in photochemical studies', International Journal of Environmental Analytical Chemistry, 85: 4, 281 — 291

To link to this Article: DOI: 10.1080/03067310412331303208

URL: http://dx.doi.org/10.1080/03067310412331303208

Intern. J. Environ. Anal. Chem.
Vol. 85, No. 4–5, 10 April–20 April 2005, 281–291

Solid-phase microextraction as a powerful tool in photochemical studies

MARTA LORES*, LUCÍA SÁNCHEZ-PRADO, MARÍA LLOMPART,
CARMEN GARCÍA-JARES and RAFAEL CELA

Departamento de Química Analítica, Nutrición y Bromatología, Facultad de Química,
Instituto de Investigación y Análisis Alimentario (IIAA), Universidad de Santiago de
Compostela, Avda. das Ciencias S/N, Campus Sur. E-15782, Santiago de Compostela, Spain

(*Received 7 June 2004; in final form 27 July 2004*)

The advantages of using solid-phase microextraction (SPME) fibres as a support for photochemical studies (photo-SPME) are discussed in this paper. This technique has been applied to a variety of environmental pollutants, permitting the simultaneous analysis of primary compounds and photoproducts. The photodegradation pathways, identity and photochemical behaviour of photoproducts and several kinetic parameters have been determined for emergent (polycyclic and nitro musks) or well-established environmental substances of concern (PCBs, PBDEs, PAHs and pesticides). Aqueous photodegradation studies followed by SPME have also been performed and compared with photo-SPME.

Keywords: Photodegradation; Photo-SPME; UV irradiation; SPME; Environmental pollutants

1. Introduction

Photochemical reactions induced by UV or visible light take place in the atmosphere, water, soil and living organisms, playing a major role in the environment. These reactions contribute to the synthesis and degradation of many organic substances, participating in the chemical equilibrium of our planet [1]. The degradation pathways of environmental pollutants imply biotic and abiotic transformations, photodegradation being one of the most important routes. Thus, ultraviolet irradiation, or its combination with oxidizing agents, is a valid approach for the elimination of different pollutants dissolved in water [2]. However, the application of these tools depends on the photodegradation nature of the target compounds, and their photoproducts are more resistant and even more toxic than the parent compounds. The identification of photoproducts and the characterization of their toxicity, for common and emergent pollutants, may contribute to a better understanding of their behaviour in the environment.

---

*Corresponding author. Fax: +34-981595012. Email: qnmlores@usc.es

International Journal of Environmental Analytical Chemistry
ISSN 0306-7319 print: ISSN 1029-0397 online
DOI: 10.1080/03067310412331303208

Solid-phase microextraction (SPME) is a suitable technique that has been successfully applied to the extraction and concentration of most environmental pollutants in different matrices [3]. This 'green' technique is simple, fast and inexpensive; requires minimum sample handling and low solvent consumption; and consequently generates a low waste output, but still provides very low detection limits and a high sensitivity and selectivity.

In classical photodegradation studies, the whole sample is irradiated before the extraction of photoproducts and liquid–liquid extraction is usually performed. This limits their efficacy, because the sensitivity is insufficient to extract low concentrations of photoproducts, thus necessitating a powerful preconcentration step. Moreover, this technique is slow, requires a high solvent consumption and, consequently, a high waste output, and is a multistep approach, increasing the possibility of losing photoproducts as the number of extractions increases. Solid-phase extraction (SPE) [4–10] is sometimes used in photochemical studies to overcome some of the aforementioned disadvantages, and SPME can be used also for extraction purposes [11–15] as will be shown below.

In this article, a different application of this extraction technique is proposed, using it as a support for photochemical studies (photo-SPME) of a variety of environmental pollutants [11–13,16–18]. In photo-SPME, first the target analytes are extracted, and then the photolysis takes place directly on the fibre, so the whole system (primary compounds and photoproducts) can be analysed simultaneously. All photoproducts will be generated directly in the SPME coating, thus obviating further extraction steps and facilitating their identification, because of the high concentration factors. Gas chromatography (GC) coupled with ion trap mass spectrometry (MS) or tandem mass spectrometry (MS/MS) has been used to monitor the degradation kinetics and to tentatively identify the photoproducts generated *in situ*. The goals of this article are to show the potential of photo-SPME in photochemical studies, to summarize the 'state of the art' and to present the new trends and advances in this technique. The photochemical behaviour in SPME fibres, both in mixtures or individually, of 39 different pollutants (polychlorinated biphenyls (PCBs), pesticides, polycyclic aromatic hydrocarbons (PAHs), musks and polybrominated diphenyl ethers (PBDEs)) has been studied recently in our laboratory. On-fibre photodegradation data for PAHs, PBDEs and triclosan are revealed for the first time in this article.

In a more classical approach, aqueous photodegradation experiments have also been carried out in all the studied pollutants, but using SPME as an alternative extraction technique, with all the inherent advantages that have already been mentioned. These results have been compared with those obtained by means of photo-SPME.

2. Experimental

The confirmation of 'on-fibre' photodegradation is the first step in photo-SPME studies. The preliminary experiments, shown in the flow diagram in figure 1, involve submitting aliquots of a water sample spiked with the desired analytes (always in concentration orders of ng/mL) to four different treatments: a control SPME extraction (no irradiation), where the fibre is directly injected into the GC without further pre-treatment; a UV irradiation exposure (photo-SPME); and dark and thermal tests to ensure that any changes in analytical response are due to the action of photons, and that volatilization or thermal degradation does not lead to any significant losses.

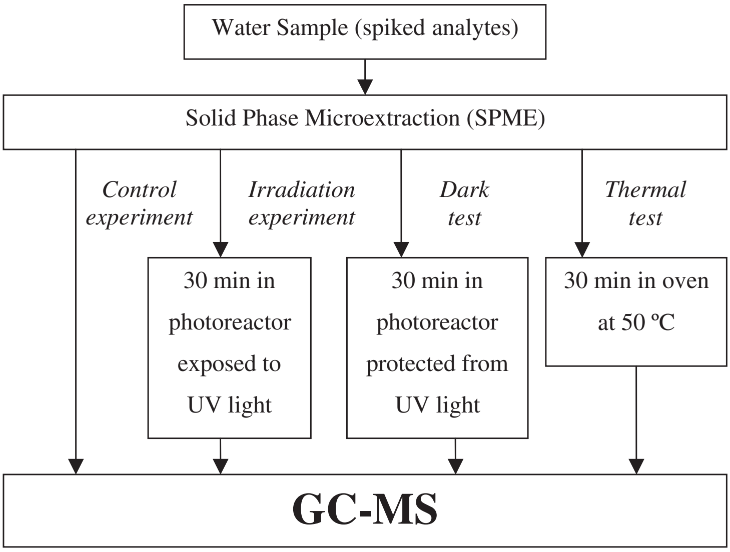

Figure 1. Flow diagram of the experimental design for preliminary experiments.

In the photo-SPME experiments, a selected volume of water spiked with the target analytes is extracted by SPME or headspace-SPME (HS-SPME), during the extraction time selected and at a constant temperature. Then, the fibre is exposed to UV radiation (254 nm) for the selected period of time in the photoreactor. The photochemical reactor, built with low-pressure mercury lamps (8–10 W), has been developed in our laboratory based on previous prototypes [19,20]. The dark test was conducted by placing the fibre, with the corresponding compounds absorbed, inside a glass vial and covering the whole device with aluminium foil; the irradiation and analysis conditions were as previously described. In the thermal test, a lab heater maintained the temperature at 50°C, high enough since in the photoreactor it never differs from the ambient value by more than ±1°C due to the cooling devices.

The fibre is finally desorbed in the chromatographic system and GC–MS or GC–MS–MS analyses were performed for the four treatments. Table 1 summarizes the GC methods used (with a Varian 3800C GC and a 1079 split/splitless injector) in each particular case. The mass spectrometer detector conditions, on a Varian Saturn 2000, are as follows: transferline temperature: 280°C; manifold temperature: 50°C; trap temperature 250°C, except for polycyclic musks (200°C) and pesticides (120°C). The mass range has been selected for each group of compounds, depending on their molecular weight and the expected characteristics of their photoproducts (when information was available) to screen for degradation products with structures closely related to that of the parent compounds and to obtain information on characteristic fragments of the degradation products. The environmental pollutants studied were extracted by HSSPME at 100°C, except pesticides (for these, extraction was carried out by direct SPME at ambient temperature). Solutions were stirred in all cases.

Aqueous photodegradation experiments have also been carried out, using quartz precision cells. In these experiments, aliquots of the water solution containing the target analytes were exposed to UV irradiation for different periods of time, and then (HS)SPME GC–MS analyses were performed.

Table 1. GC conditions for each group of environmental pollutants investigated.

	GC conditions: Varian 3800 C with a 1079 split/splitless injector			
	Column	Injector temperature (°C)	Oven program	Carrier gas, helium
PCBs	CPSil-8, 25 m × 0.32 mm i.d., 0.25 μm	270	60°C, 2 min; 20°C/min; 170°C, 6 min; 3°C/min; 280°C, 10 min	1.0 mL/min
PAHs	BP1, 25 m × 0.32 mm i.d., 0.17 μm	270	60°C, 1 min; 10°C/min; 260°C, 5 min	1.4 mL/min
DDT, DDD and DDE		270	60°C, 2 min; 15°C/min; 115°C; 3°C/min; 175°C, 30°C/min; 250°C, 2 min; 5°C/min; 280°C, 10 min	1.4 mL/min
Policyclic musks and Nitro musks	VA-5MS, 25 m × 0.25 mm i.d., 0.25 μm	270	40°C, 2 min; 15°C/min; 280°C, 5 min	10.3 kPa (1.5 psi), 0.93 min; 2.8 kPa/min (0.41 psi/min); 58.6 kPa (8.5 psi), 5 min
Atrazine, alachlor, aldrin, dieldrin, endrin and triclosan	CPSil-8, 30 m × 0.25 mm i.d., 0.25 μm	280	55°C, 2 min; 8°C/min; 210°C, 20 min; 10°C/min; 280°C	1.2 mL/min
PBDEs			60°C, 2 min; 30°C/min; 250°C; 5°C/min; 280°C, 8 min	1.2 mL/min

2.1. *SPME coatings in photo-SPME*

Different commercial fibre coatings (Supelco, Bellefonte, PA) have been tested to establish the viability of performing on-fibre photodegradation studies. For all the pollutants and under the selected irradiation conditions, on-fibre photodegradation took place only on polydimethylsiloxane (PDMS). With other coatings such as carboxen-PDMS (CAR-PDMS), PDMS-divinylbenzene (PDMS-DVB), polyacrylate (PA) or carbowax-DVB (CW), GC–MS responses indicated that the extent of photodegradation was very limited or nonexistent. As an example, experiments recently carried out with four polycyclic aromatic hydrocarbons, fluorene, anthracene, pyrene, and benzo(a) pyrene, have also confirmed the PDMS 'on-fibre' photodegradation for this kind of compound. Figure 2 shows the results obtained for anthracene. PDMS was used in all the remaining experiments as the coating support in the photochemical studies.

2.2. *Kinetic parameters*

Kinetic parameters can be easily calculated by photo-SPME: the apparent first-order rate constants (k_{ap}) can be determined as the slopes of the straight-line equations

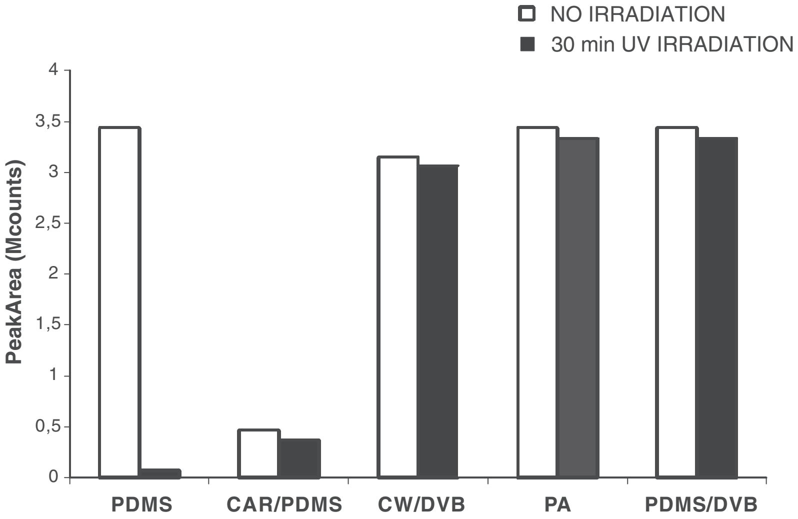

Figure 2. Effect of 30 min of UV irradiation (254 nm) on the anthracene peak areas on different fibre coatings: polydimethylsiloxane (PDMS), 100 µm; carboxen-PDMS (CAR-PDMS), 74 µm; PDMS-divinylbenzene (PDMS-DVB), 65 µm; polyacrylate (PA), 85 µm; and carbowax-DVB (CW), 65 µm. Experimental conditions: HSSPME at 100°C for 15 min; analyte concentration 20 ng/mL; quantification ion (*m*/*z*) 178.

obtained from linear regression: $\ln C$ *vs.* time plot. The corresponding half-lives (when the reagent species concentration is reduced to 50% of its initial amount) are calculated using this expression:

$$t_{1/2} = \ln 2/k_{\mathrm{ap}}$$

The total reaction order (n) is calculated by the 'half-life time comparison method':

$$n = 1 + \frac{\ln(t_{1/2}) - \ln(t_{1/2})}{\ln C_2 - \ln C_1}.$$

3. Results and discussion

3.1. *Preliminary experiments*

Each treatment (photo-SPME, dark test and thermal test) was compared with the control, showing that only photodegradation experiments have led to significant peak area decrements. Experimental results showed that the dark reactions were negligible. Even in the most volatile analytes, where some losses can occur (note that the thermal test is carried out under forced conditions), it is clear that photodegradation is the main reaction (figure 3). This is the case for PCBs 28 and 31, coeluting trichlorobiphenyls, and PCB 52, the less reactive among the studied congeners due to its substitution pattern [11,16].

3.2. *Influence of irradiation time and kinetic studies*

Once it has been demonstrated that the studied compounds are photochemically degradable, peak area changes for each individual compound after UV exposure can

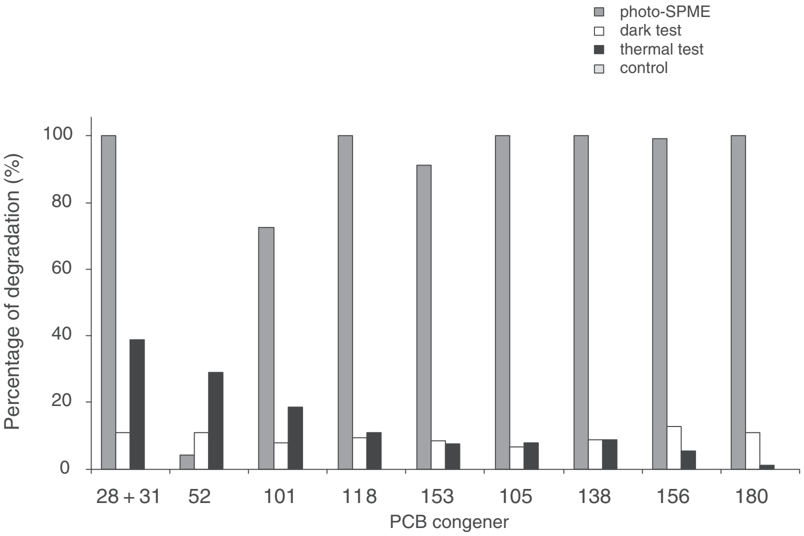

Figure 3. Percentage of degradation in preliminary experiments for 10 PCBs congeners ranging from three to seven chlorine substituents (note that in the control experiments, the degradation is 0% in all cases).

be evaluated, as shown in the chromatograms of PBDEs for two selected irradiation times (figure 4). On-fibre photodegradation of these brominated flame retardant chemicals is demonstrated for the first time in these initial studies, where the remainder of the initial compounds after 60 min of UV irradiation is less than 1%.

Then, by plotting the percentage of undegraded compound *vs*. irradiation time, the photodegradation kinetic curves are obtained (figure 5). In this example, four nitro musks show comparable photodegradation behaviours. Photochemical reactions follow first-order kinetics, indicating that the decrease in reagent concentration is an exponential function of irradiation time. Up to now, the most exhaustive discussion of kinetic parameters using photo-SPME has been done for nitromusks [13]. The apparent first-order rate constants (k_{ap}), in the order of 10^{-4} s^{-1}, were similar, irrespective of the initial concentration (see average experimental data in figure 5), as would be expected in first-order reactions and as confirmed by the total reaction order values close to unity for all the nitrated musk compounds.

3.3. *Photoproducts*

A large number of photoproducts were detected in these experiments, and these were tentatively identified on the basis of their mass spectra and sometimes using the information found in the literature. Since quite a number of isomers were identified, structures of the degradation products were proposed by considering the most likely fragmentation patterns in MS or MS/MS experiments. Eleven and 31 dehalogenated photoproducts were obtained from the PCBs [11,16] and PBDES photodegradation studies, respectively. From PAHs, just eight new compounds could be determined under the experimental conditions, among them photogenerated ketones, as anthracenedione and dibenzo[b,e]oxepin-11(6H)-one from anthracene and 9h-fluoren-9-one from fluorene. Fifteen different transformation products were obtained in the photo-SPME of DDT, DDE and DDMU [12]; 14 from nitro musks [13], 30 from

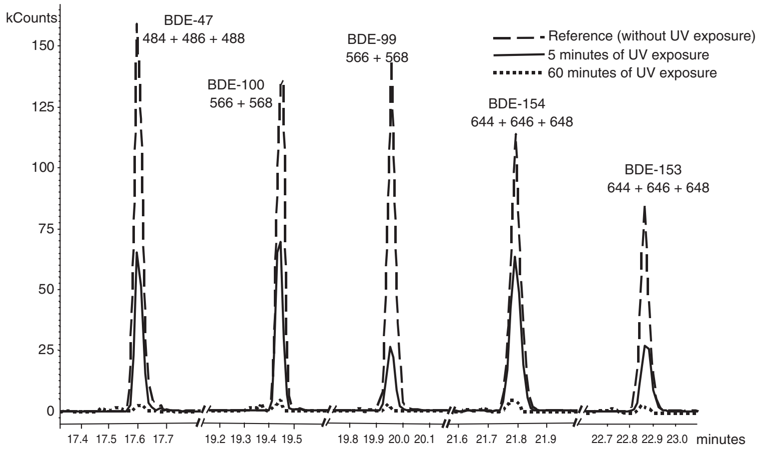

Figure 4. Overlaid quantification ion chromatograms obtained for the control (no irradiation) and for two selected UV irradiation times (5 and 60 min) of five PBDE congeners: one tetrabromodiphenyl ether (BDE-47); two pentabromodiphenyl ethers (BDE-99 and BDE-100); and two hexabromodiphenyl ethers (BDE-153 and BDE-154). Experimental conditions: HSSPME at 100°C for 30 min; total analyte concentration 5 ng/mL; quantification ions (*m*/*z*) depicted.

Compound		
Xylene	k_{ap} (s^{-1})	0,00075
	$t_{1/2}$ (s)	954
	n	0,98
Moskene	k_{ap} (s^{-1})	0,00065
	$t_{1/2}$ (s)	1150
	n	0,93
Tibetene	k_{ap} (s^{-1})	0,00045
	$t_{1/2}$ (s)	1710
	n	0,93
Ketone	k_{ap} (s^{-1})	0,0006
	$t_{1/2}$ (s)	1192
	n	1,03

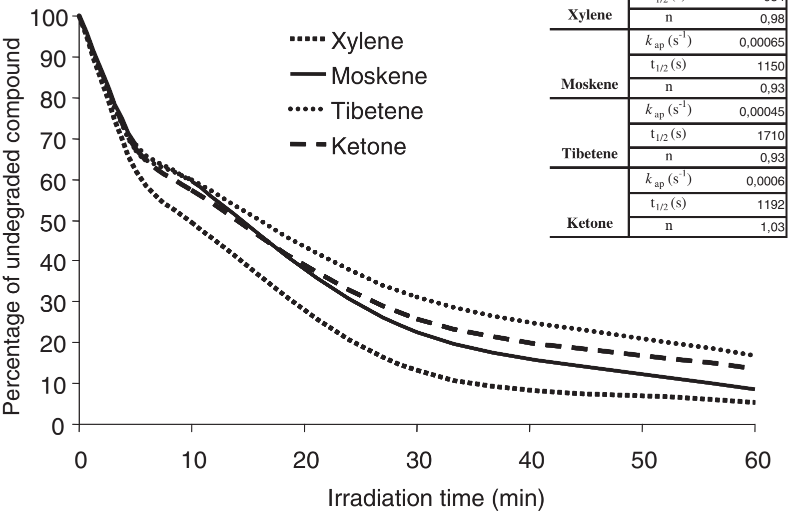

Figure 5. Photodegradation kinetic curves of nitro musks obtained in photo-SPME experiments. The corresponding average kinetic parameters, apparent first-order rate constants (k_{ap}), half-life times ($t_{1/2}$) and reaction orders (n), are shown in the insert.

polycyclic musks [17] and more than 60 from the pesticide-irradiation experiments [18]. The proposed identity of some of these new generated compounds matched the photoproducts structures suggested for other authors. In some other cases (e.g. the nitromusks moskene and tibetene or the six polycyclic musks studied), no previous studies concerning photodegradation pathways could be found.

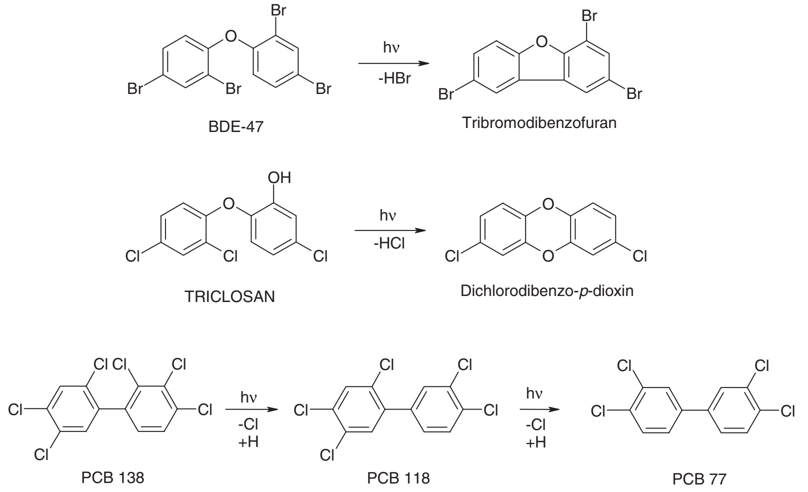

Figure 6. Three examples of UV-induced photochemical reactions that led to photoproducts more toxic than the native compounds.

The phototransformation of these non-spiked compounds was easy to follow thanks to the potential of GC–MS. The obtained formation-photodegradation kinetic curves showed three different behaviours: (1) some photoproducts were detected after short irradiation times and became undetectable at longer UV expositions; they can be considered as being easily photodegradable; (2) other photoproducts were hardly photodegradable during the evaluated time period; and (3) there was a group of photoproducts which showed an intermediate behaviour. This performance could be related to their chemical structural in some cases (e.g. PCBs and PBDEs).

Besides characterizing the photochemical persistence of the by-products, it is also important to evaluate their toxicity, and we found several cases where the photoproducts were more toxic than the starting compounds (figure 6): (1) two dibromodibenzofurans and one tribromobenzofuran have been identified as photoproducts of PBDEs; (2) the photochemical conversion of triclosan into the highly toxic dichlorodibenzo-*p*-dioxin (DCDD) has been confirmed in the preliminary experiments of triclosan photodegradation using photo-SPME (a polemic photoformation because it seems to primary depend on the experimental conditions); (3) several specific PCB coplanar congeners that are structurally related to 2,3,7,8-tetrachlorodibenzodioxin (TCDD) have toxicological properties similar to this compound. With the rapid degradation of PCB 138, the toxic coplanar congener 77 is largely produced through photodegradation of PCB 118, and the toxic equivalents (TEQs) of the solution increased rapidly [11,16] (figure 6).

3.4. *Main photodegradation mechanisms*

The main photodegradation mechanisms of all studied compounds were easily deduced by photo-SPME. For PCBs and PBDEs, reductive dehalogenation is the first reaction, but in PBDEs the formation of furans by intramolecular cyclization has also been confirmed by this technique, as explained above. These two reactions, among others like oxidation, reduction, isomerization, hydroxylation and loss of alkyl radicals, have also been observed in pesticides and musks. On some occasions, the photodegradation of a particular analyte has multiple pathways simultaneously. For example, the main photoproduct of atrazine is generated through the chlorine atom loss, and this photoproduct can lose the ethyl group, an important reaction since the dechlorinated product of atrazine loses the phytotoxicity of its parent compound. However, atrazine also undergoes ethyl or isopropyl group loss or the formation of a hydroxylated photoproduct.

3.5. *SPME as an extraction alternative in aqueous photochemistry*

Aqueous photodegradation experiments have also been carried out for every studied compound, using SPME as an alternative extraction technique. All of the photoproducts obtained in the aqueous photodegradation experiments were also found in the photo-SPME experiments, including the most toxic by-products. In contrast, some photoproducts identified in photo-SPME did not appear in the water experiments. This can be explained, among other reasons (e.g. role of solvent in photochemical reactions), taking into account that in 'on-fibre' photodegradation, photoproducts are generated *in situ* on the fibre without any additional steps for extraction. However, in aqueous photodegradation studies, photoproducts are generated in the solution, and they must be extracted by SPME. In most cases, the behaviour of the analytes in these aqueous photodegradation experiments is similar to that obtained in the photo-SPME experiments [11,12,17,18], as can be seen for four polycyclic musks in figure 7.

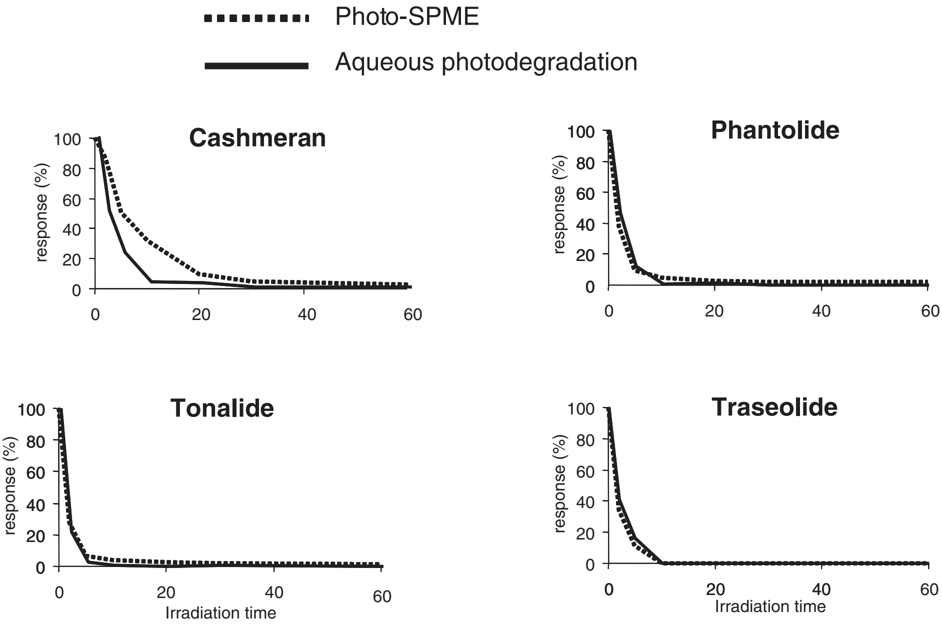

Figure 7. Photo-SPME *vs.* aqueous photodegradation of four polycyclic musks.

4. Concluding remarks

SPME is a very convenient technique that simplifies the photochemical studies of environmental organic pollutants. In summary, the main applications of the photo-SPME approach are the acquisition of photodegradation curves of primary compounds, their kinetic parameters, their main and secondary photodegradation pathways, and identification and photochemical behaviour of their photoproducts. These applications are well established and reported for a number of different environmental pollutants. Thus, when the photochemical behaviour of a particular group of analytes needs to be known, photo-SPME can be used.

Besides, SPME can be used as an extraction technique to study the photochemical process in matrices other than the SPME coating (e.g. water) in a more classical approach, extraction after irradiation, but with all the above-mentioned advantages of this 'green technique'. In most of the compounds studied, photo-SPME mimics the photochemical behaviour of the pollutants in water samples quite well.

5. Future trends

Among the fundamental aspects of the technique, it is important to establish the reasons for why photo-SPME works much better on PDMS fibres than in other coatings; fluorescence microscopy will help in this subject. To better mimic the photochemical behaviour of these pollutants under solar irradiation but in controlled conditions, solar simulator studies are needed. The use of portable SPME devices to undertake photodegradation studies in the field under the natural changing conditions is also an attractive topic. Doping of the fibre with sensitizers or radical initiators will help to evaulate photo-SPME under these conditions. Finally, photoderivatization processes can increase the sensitivity and selectivity of the detection. Some of these aspects will be investigated in the near future.

Acknowledgements

This research was supported by the projects BQU2002-01944 and BQU2003-02090 from the CICYT (Ministerio de Ciencia y Tecnología, Spain) and PGIDIT03PXIC23701PN and PGIDIT04PXIC23701PN from Xunta de Galicia. L. Sánchez-Prado would like to acknowledge her grant to the CICYT.

References

[1] P. Boule (Ed.), *Environmental Photochemistry*, p. XIII, Springer, Berlin (1999).

[2] M.M. Halmann, *Photodegradation of Water Pollutants.* CRC Press, Boca Ratón, FL (1996).

[3] J. Pawliszyn, *Applications of Solid Phase Microextraction.* R.S.C. Chromatography Monographs. The Royal Society of Chemistry, Cambridge (1999).

[4] A.D. Dimou, V.A. Sakkas, T.A. Albanis, *J. Photochem. Photobiol. A*, **163**, 473 (2004).

[5] A. Farran, S. Ruiz, *J. Chromatogr. A*, **1024**, 267 (2004).

[6] M. Castillo, G. Penuela, D. Barceló, *Fresenius J. Anal. Chem.*, **369**, 620 (2001).

[7] G.A. Penuela, I. Ferrer, D. Barceló, *Int. J. Environ. Anal. Chem.*, **78**, 25 (2000).

[8] S. Chiron, J.A. Torres, A. Fernández-Alba, M.F. Alpendurada, D. Barceló, *Int. J. Environ. Anal. Chem.*, **65**, 37 (1996).

[9] D. Barceló, S. Chiron, A. Fernández-Alba, *Organohalogen Comp.*, **24**, 517 (1995).

[10] S. Chiron, J. Abian, M. Ferrer, F. Sánchez-Baeza, A. Messeguer, D. Barceló, *Environ. Toxicol. Chem.*, **14**, 1287 (1995).

[11] M. Lores, M. Llompart, R. González-García, C. González-Barreiro, R. Cela, *J. Chromatogr. A*, **963**, 37 (2002).

[12] M. Llompart, M. Lores, M. Lourido, L. Sánchez-Prado, R. Cela, *J. Chromatogr. A*, **985**, 175 (2003).

[13] L. Sánchez-Prado, M. Lores, M. Llompart, C. García-Jares, M. Lourido, R. Cela, *J. Chromatogr. A*, **1048**, 73 (2004).

[14] T.M. Sakellarides, V.A. Sakkas, D.A. Lambropoulou, T.S.A. Albanis, *Int. J. Environ. Anal. Chem.*, **84**, 161 (2004).

[15] M.J. Bernhard, S.L. Simonich, *Environ. Toxicol. Chem.*, **19**, 1705 (2000).

[16] M. Lores, M. Llompart, R. González-García, C. González-Barreiro, R. Cela, *Chemosphere,* **47**, 607 (2002).

[17] L. Sánchez-Prado, M. Lourido, M. Lores, M. Llompart, C. García-Jares, R. Cela, *Rapid Commun. Mass. Spectrom.*, **18**, 1186 (2004).

[18] L. Sánchez-Prado, M. Llompart, M. Lores, C. García-Jares, R. Cela, *J. Chromatogr. A*, **1047**, 771 (2004).

[19] R. Cela, M. Lores, C.M. García, *J. Chromatogr. A*, **626**, 117 (1992).

[20] M. Lores, R. Cela, C.M. García, *J. Chromatogr. A*, **724**, 55 (1994).